Optimum Design of continuous composite slab using Particle Swarm Optimization

Mariana Oliveira Teixeira[1], Élcio Cassimiro Alves[1], Janaina Pena Soares de Oliveira Valle[2], Adenilcia Fernanda Grobério Calenzani[1]

[1] Universidade Federal do Espírito Santo - UFES, Department of Civil Engineering,
Vitória, Espírito Santo, Brazil
[2] Instituto Federal do Espírito Santo – IFES, Department of Civil Engineering,
Vitória, ES, Brasil
mariana.oliveiratx@gmail.com, elcio.alves@ufes.br, janaina.pena@ifes.edu.br, *afcalenzani@gmail.com.*

Abstract: Civil construction is one of the main contributors to the emission of CO_2 in the atmosphere. In the pursuit of more environmentally friendly structures, evaluating the emission of gases generated by civil construction, particularly in the manufacturing process of composite slabs, is of paramount importance. Composite slabs are typically analyzed as a succession of simply supported spans; however, due to the construction method, these structures are actually built as continuous. Considering the continuity of the slabs in composite steel and concrete systems can lead to a more optimized structural design. The aim of this paper is to determine optimal solutions for continuous composite slabs in terms of CO_2 emissions. The constraints of the optimization problem are based on the design criteria of Brazilian Standards, and the solution to the optimization problem was obtained using Particle Swarm Optimization. As result, the algorithm selected slabs with thinner steel formwork, lower concrete cover, and lower rates of negative and additional positive reinforcement. Additionally, it chosen concrete with intermediate compressive strength and a rate of negative reinforcement close to lower bound. The CO_2 emissions resulting from steel formwork and concrete were the most influential variables in the final problem solution.

Keywords: continuous composite slabs; optimization; particle swarm algorithm; additional reinforcement; negative reinforcement.

1 Introduction

Achieving the perfect balance between performance and sustainability is crucial in today's civil construction industry. This is particularly important as civil construction stands as one of the leading contributors to CO2 emissions in the economic sector. Consequently, extensive research has been conducted to explore methods of minimizing greenhouse gas emissions, aiming for enhanced environmental performance. Composite slabs represent structural elements replete with numerous advantages. These advantages include self-support during concreting, ease of installation, and a reduction in the formwork needed for construction. In recent years, continuous composite slabs have been studied as exemplified in research by ABAS *et al.* [1], TIAN *et al.* [2], Bolina *et al*. [3] and ZHANG *et al.* [4]. Many authors have used optimization to find the best solutions with an emphasis on economy and sustainability. The use of metaheuristic algorithm as Particle Swarm Optimization (PSO) proposed by Kennedy and Eberhart [5], is widely adopted due to its ease of implementation and good performance. Authors like Poitras *et al.* [6], Lin *et al.* [7] and Vosoughi and Gerist [8] have employed PSO as their chosen optimization algorithm.

The study of continuous composite slabs is a recently emerging research area, and the analysis of their optimization with a focus on environmental impact promises to yield significant benefits for the civil construction industry. Consequently, this research presents the formulation of the optimization problem for continuous composite slabs, taking into account their environmental impacts by evaluating CO_2 emission during the manufacturing process. Additionally, this study evaluates the use of additional positive reinforcement based on research by Grossi *et al*. [9], as well as determining the required negative reinforcement ratio in the vicinity of the supports.

2 Optimization Problem Formulation

2.1 Design Variables

The design variables considered in the optimization problem include the following: the thickness of the concrete above the formwork ($x_1 = t_c$), the characteristic compressive strength of concrete ($x_2 = f_{ck}$), the thickness of the steel formwork ($x_3 = t_f$), the additional positive reinforcement ratio ($x_4 = \rho_R$), the type of steel formwork according to the manufacturer (x_5), the negative reinforcement ratio ($x_6 = \rho_{NR}$), and the diameter of the negative reinforcement ($x_7 = \rho_{\phi NR}$). Figure 1 illustrates the composite slab with the design variables indicated, and Fig. 2 represents the formwork analyzed in this study, Polydeck 59S.

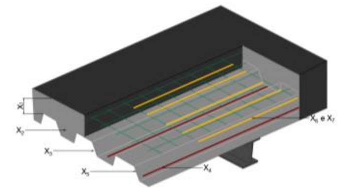

Figure 1. Continuous composite slab with its variables.

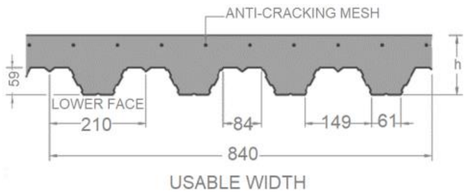

Figure 2. Steel forms Polydeck 59S [10].

2.2 Objective Function

To discover the optimal solution with regards to the environmental impacts associated with the construction of continuous composite slabs, the objective function is employed as per eq. 1. This function aims to yield the outcome with the lowest total CO_2 emissions, derived from the emission of each component of the composite slab.

$$Min\ CO_2 = Em_{\mathrm{Sd}} + Em_{\mathrm{C}} + Em_{\mathrm{R}} + Em_{\mathrm{w}} + Em_{\mathrm{NR}} + Em_{Cr} \quad (1)$$

where Em_{Sd}, Em_{C}, Em_{R}, Em_{W}, Em_{NR} and Em_{Cr} correspond to CO_2 emissions, measured in $kgCO_2$, originating from steel formwork, concrete, additional positive reinforcement, shrinkage-induced cracking, negative reinforcement, and cracking reinforcement, respectively. The CO_2 emission values for concrete and steel were proposed by Santoro e Kripka [11] and Worldsteel Association [12], respectively, and are detailed in Tab. 1.

Table 1. CO_2 emission in concrete production

Component	Strength	CO_2 Emission ($kgCO_2/m^3$)	Source
Concrete	20 MPa	129.85	Santoro and Kripka [11]
	25 MPa	142.71	
	30 MPa	153.68	
	35 MPa	163.25	
	40 MPa	171.73	
	45 MPa	189.60	
	50 MPa	199.72	
Steel formwork	280 MPa	2.6380	Worldsteel Association [12]
Additional reinforcement Wire mesh Cracking reinforcement Negative bending reinforcement	600 MPa	1.9240	

2.3 Constraints

Eight design constraints were defined based on the sizing criteria established by ABNT NBR 8800 [13], which are as follows:

$$C(1): \frac{M_{Sd}^{+}}{M_{Rd}^{+}} - 1 \leq 0 \quad (1)$$

$$C(2): \frac{V_{Sd}}{V_{v,Rd}} - 1 \leq 0 \quad (2)$$

$$C(3): \frac{V_{Sd}}{V_{l,Rd}} - 1 \leq 0 \quad (3)$$

$$C(4): \frac{\delta}{\delta_{máx}} - 1 \leq 0 \quad (4)$$

$$C(5): \frac{M_{Sd}^{-}}{M_{Rd}^{-}} - 1 \leq 0 \quad (5)$$

$$C(6): \frac{esp_{NR}}{esp_{máx}} - 1 \leq 0 \quad (6)$$

$$C(7): 1 - \frac{esp_{NR}}{esp_{min}} \leq 0 \quad (7)$$

$$C(8): 1 - \frac{\phi_{NR}}{t_c/8} \leq 0 \quad (8)$$

The constraints pertain to the limit states concerning positive bending moment, $C(1)$, vertical shear, $C(2)$, and longitudinal shear, $C(3)$. Constraint $C(4)$ ensures compliance with the excessive deflection service limit state, while $C(5)$ monitors limit states associated with negative bending moment. The spacing of the negative reinforcement bars is assessed against the maximum and minimum allowable spacing in constraints $C(6)$ and $C(7)$, respectively. Finally, constraint $C(8)$.guarantees that the maximum diameter limit for this reinforcement is upheld.

3 Results and Discussions

In this study, continuous composite slabs were constructed using a steel formwork, specifically Polydeck 59S from the Perfilor catalog [10]. The analysis was conducted with 2 spans, each measuring 3.4 m, and the loads were defined as per the manufacturer's specifications. The material properties were as follows: the modulus of elasticity of steel (E_a) was 200 GPa, the specific mass of steel was 7850 kg/m³, and the strength weighting factor were 1.4 for concrete (γ_c), 1.15 for steel formwork (γ_a), 1.15 for reinforcement (γ_{sl}) and 1.43 for longitudinal shear strength(γ_{sl}). In the optimization problem, the design variables were considered as discrete, and the define ranges for each variable were as follows: t_c ranged from 51 to 191 mm, with increment of 10 mm; the f_{ck} ranged from 20 to 50 MPa with an increment of 5 MPa; three options for t_f were considered: 0.8 mm, 0.95 mm and 1.25 mm; ρ_R varied from 0% to 0.25%, with an increment of 0.05%; ρ_{NR} ranged from 0.15% to 4%, with increment of 0.05%; and five possibilities for the diameter of the welded cracking reinforcement, denoted as ϕ_{NR}, with values of 3.8, 4.2, 5, 6.3 and 8 mm. Tab. 2 presents the load cases that were analyzed. These values were utilized to optimize the composite slabs based on CO_2 emissions.

Table 2. Load cases analyzed.

Load case	kN/m²	Load case	kN/m²	Load case	kN/m²	Load case	kN/m²	Load case	kN/m²	Load case	kN/m²
1	4.45	9	8.62	17	4.87	25	4.51	33	10.48	41	7.36
2	5.16	10	3.34	18	10.81	26	5.8	34	5.22	42	12.06
3	7.14	11	4.26	19	4.04	27	9.43	35	6.74	43	5.94
4	2.88	12	9.35	20	5.18	28	4.75	36	11.00	44	7.68
5	5.69	13	3.57	21	11.55	29	6.11	37	5.46	45	12.58
6	7.89	14	4.57	22	4.27	30	9.96	38	7.05	-	-
7	3.11	15	10.08	23	5.49	31	4.98	39	11.53	-	-
8	6.21	16	3.8	24	12.29	32	6.42	40	5.7	-	-

As an example, Tab. 3 presents the optimal solution that was found, along with the corresponding result from the manufacturer's catalog for load case 42.

Table 3. Comparing the manufacturer's result to the optimized solution

Solution	Properties							
	h_t (mm)	h_f	t_c (mm)	t_f (mm)	f_{ck} (MPa)	ρ_R (%)	ρ_{NR}	Load (kN/m²)
Manufacturer	240	59	181	1.25	20	0	TS246	12.06
Authors PSO	150	59	91	0.8	40	0.15	0.4%	12.06
Solution	CO_2 Emission							
	Formwork	Concrete	Addition reinforcement	Wire mesh	Negative reinforcement	Cracking Reinforcement	Total	Manufacturer/ Optimization
Manufacturer ($kgCO_2$)	256.34	182.78	0	28.78	8.63	0	476.53	140 %
Authors PSO ($kgCO_2$)	163.96	136.94	14.02	15.83	10.32	0	341.07	

According to Tab. 3, it is evident that, for equivalent load levels, the manufacturer's total CO_2 emissions were 40% higher than those of the optimized solution. It is worth noting that the optimized solution employed a steel formwork with a thickness of 0.8 mm, which happened to be the most significant contributor to the overall CO_2 emissions. Additionally, the optimized solution utilized concrete with a strength of 40 MPa and reduced the thickness of the concrete layer. It also incorporated additional positive reinforcement at a rate of 0.15% and negative reinforcement at 0.4%. These choices underscore the advantages of using reinforcement elements to enhance the slab's load-bearing capacity with minimal impact on CO_2 emissions. Many components contributing to the total CO_2 emissions of the slab were effectively reduced. Specifically, the emissions per element in the manufacturer's solution were 56.3% higher for the formwork, 33.5% for the concrete, and 81.8% for cracking reinforcement. In contrast, the negative reinforcement in the manufacturer's design was 16.3% less than that in the optimization algorithm. Figure 3 illustrates the ratio between the CO_2 emissions of the manufacturer's solutions and the optimized ones, emphasizing the significant reductions achieved through the optimization process.

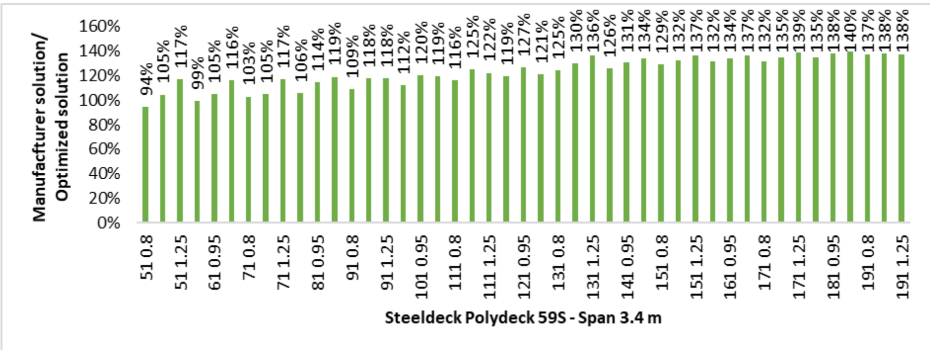

Figure 3. Ratio between issuance of CO_2 - Manufacturer's solution / Optimized solution for span 3.4 m

As illustrated in Fig. 3, the optimal solutions generally outperformed the manufacturer's proposed solutions, with just two exceptions. In these cases, the algorithm considers as the best solution the use of a concrete with f_{ck} equivalent to 35 and 30 MPa, which offer greater durability compared to the concrete of 20 MPa. It is worth noting that the manufacturer's catalog specifies an f_{ck} value of 22 MPa, but for the emissions analysis it was considered an f_{ck} of 20 MPa, as the associated CO_2 emissions for this f_{ck} value were provided and documented in Tab. 1.

It is evident that for higher load values, the optimization yielded superior results compared to those offered by the manufacturer, demonstrating its efficiency in handling higher load situations. Additionally, Fig. 3 illustrates that the manufacturer's emissions are up to 40% higher than those determined by the algorithm. Figure 4 provides a breakdown of the CO_2 emissions associated with each component of the continuous composite slab.

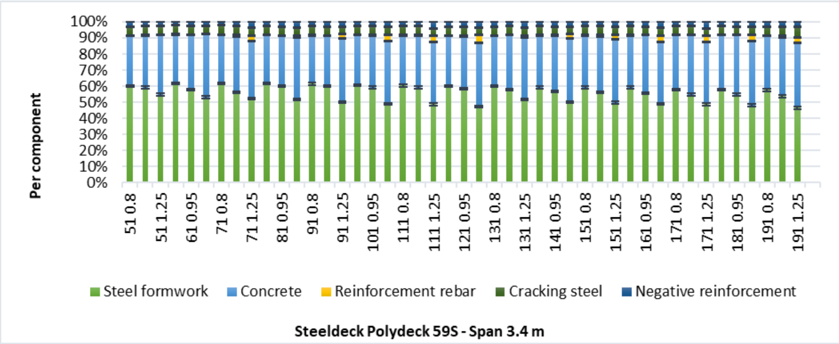

Figure 4. CO_2 emission per component of the Polydeck 59S with a span of 3.4 m

As Fig. 4 illustrates, the slab formwork was the element with the greatest contribution to the total CO_2 emission of the structure, followed by the concrete, cracking reinforcement, negative reinforcement and addition reinforcement. It is important to observe that the positive reinforcement addition has its importance, by helping to reduce the thickness of the formwork and the overall CO_2 emission of the structure. Figure 5 provides an overview of the optimization constraints, with the dimensioning of the slabs primarily governed by criteria such as longitudinal shear force and the negative bending moment.

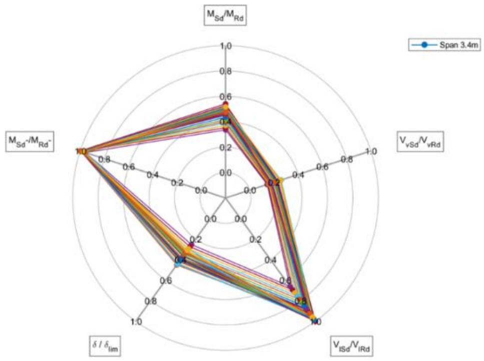

Figure 5. Analysis of constraints for continuous slabs and spans of 3.4 m

Figures 6 to 11 present an analysis of the parameters that had the most significant impacted on the optimization of the proposed problem, including the thickness of the concrete cover, formwork, positive and negative reinforcement ratio, characteristic strength of concrete and negative reinforcement diameter.

As show in Fig. 6, it is clear that the most commonly concrete cover height was 51 mm. This selection aligns with the goal of minimizing the concrete volume since it represents the smallest volume among the available options. Notably, the formwork thickness remained constant at 0.8 mm across all load cases. Recognizing that this component substantially contributes to CO_2 emissions, our optimization solution was designed to prioritize reducing formwork thickness while still meeting the problem's constraints. This approach ultimately led to minimal utilization of steel formwork volume, as depicted in Fig. 7.

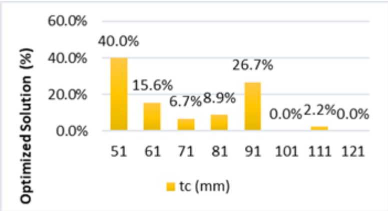

Figure 6. Concrete cover height

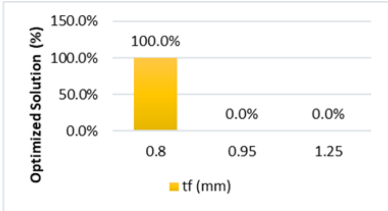

Figure 7. Thickness of steel formwork

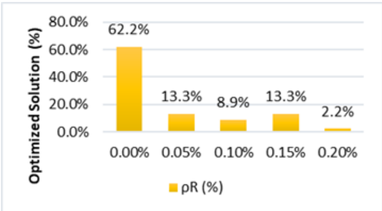

Figure 8. Selected positive reinforcement rate

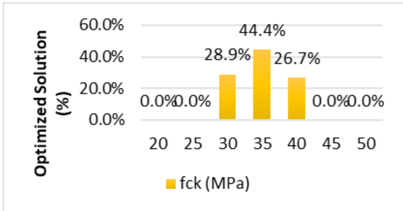

Figure 9. Characteristic strength of concrete

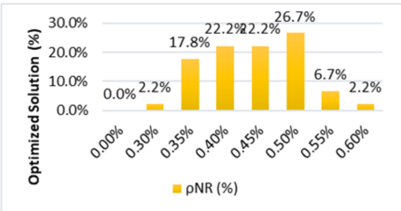

Figure 10. Negative reinforcement rate selected

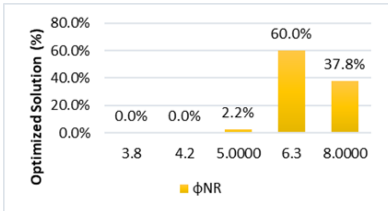

Figure 11. Negative reinforcement diameter

Figure 8 reveals that the algorithm excluded additional positive reinforcement in 62.2% of cases due to the redistribution of positive moments, reducing the need for extra positive reinforcement and formwork alone can withstand the stresses. While this choice has a limited impact on CO_2 emissions, it enhances the flexural strength of the slab without requiring thicker steel formwork, as illustrated. As shown in Fig. 9, the most frequently chosen characteristic concrete strength was 35 MPa. When we compare this with Fig. 6, it becomes evident that the preference for smaller concrete covers necessitated the use of higher f_{ck} values. Intermediate values were selected to ensure that the concrete could withstand compression forces without significantly increasing CO_2 emissions. In Fig. 10 and 11, it is worth noting that the most commonly used negative reinforcement rate was 0.5%, paired with a steel bar diameter of 6.3 mm. The choice of a 6.3 mm diameter aligns with the maximum diameter criteria determined by the concrete cover.

4 Conclusions

After analysis results, it becomes evident that 40% of these solutions featured the lowest possible concrete cover height, which stood at 51 mm. This specific configuration consistently yielded lower CO_2 emissions. It's worth noting that all optimal solutions employed the thinnest steel formwork, measuring 0.8 mm, due to its lower weight and subsequently reduced CO_2 emissions. In 38.8% of cases, additional reinforcement was incorporated, leading to both a decrease in CO_2 emissions and an enhancement of the composite slab's structural integrity. In conclusion, our research's formulation and algorithm delivered optimized results that outperformed those of the manufacturer while adhering to the same design criteria and technical standards.

Acknowledgements. The authors acknowledge the Brazilian Federal Government Agency CAPES and State Agency of Espírito Santo for the financial support provided during the development of this research. The second author thanks State Agency of Espírito Santo for the productivity research grant and fourth author thanks the Brazilian Federal Government Agency CNPq for the productivity research grant number 309741/2020-3.

Authorship statement. The authors hereby confirm that they are the sole liable persons responsible for the authorship of this work, and that all material that has been herein included as part of the present paper is either the property (and authorship) of the authors or has the permission of the owners to be included here.

References

[1] Abas, F. M., Gilbert, R. I., Foster, S. J., & Bradford, M. A. (2013). Strength and serviceability of continuous composite slabs with deep trapezoidal steel decking and steel fibre reinforced concrete. *Engineering Structures*, *49*, 866-875.
[2] Tian, J., Wang, M., Liu, J., Guo, H., Wang, Z., & Zhang, J. (2021, December). Experimental and numerical study of continuous span concrete composite slabs. In *Structures* (Vol. 34, pp. 827-839). Elsevier.
[3] Bolina, F. L., Tutikian, B., & Rodrigues, J. P. C. (2021). Experimental analysis on the structural continuity effect in steel decking concrete slabs subjected to fire. *Engineering Structures*, *240*, 112299.
[4] Zhang, H., Geng, Y., Wang, Y. Y., & Wang, Q. (2020). Long-term behavior of continuous composite slabs made with 100% fine and coarse recycled aggregate. *Engineering Structures*, *212*, 110464.
[5] J. Kennedy, R. Eberhart. Particle swarm optimization. Proceedings of ICNN'95 - International Conference on Neural Networks. IEEE, 1995. p. 1942-1948. doi: 10.1109/icnn.1995.488968.
[6] G. Poitras, G. Lefrançois, G. Cormier. Optimization of steel floor systems using particle swarm optimization. *J. Constr. Steel Res.*, Moncton, vol. 67, n. 8, p. 1225-1231, 2011. doi:10.1016/j.jcsr.2011.02.016.
[7] J. P. Lin, G. Wang, R. Xu. Particle Swarm Optimization – Based Finite-Element Analyses and Designs of Shear Connector Distributions for Partial-Interaction Composite Beams. *Journal Of Bridge Engineering*, vol. 24, n. 4, p. 04019017, 2019. doi: 10.1061/(asce)be.1943-5592.0001371.
[8] A. R. Vosoughi, S. Gerist. New hybrid FE-PSO-CGAs sensitivity base technique for damage detection of laminated composite beams. *Composite Structures*, vol. 118, p. 68-73, 2014. https://doi.org/10.1016/j.compstruct.2014.07.012.
[9] L. G. F. Grossi, C. F. R. Santos, M. Malite. Longitudinal shear strength prediction for steel-concrete composite 90 slabs with additional reinforcement bars. *J. Constr. Steel Res.*, São Carlos, vol. 166, p. 105908, 2020. https://doi.org/10.1016/j.jcsr.2019.105908.
[10] Polydeck 59S. Steel deck catalogue. <http://www.perrfilor.com.br. (accessed: 10 March 2023).
[11] J. F. Santoro and M. Kripka, Minimizing environmental impact from optimized sizing of reinforced concrete elements. *Comput. Concr*., vol. 25, no. 2, pp. 111–118, 2020. https://doi.org/10.12989/cac.2020.25.2.111.
[12] Worldsteel Association. LCI data for steel products. https:// www. worldsteel.org (accessed 27 Jan 2022).
[13] ABNT NBR 8800, Design of steel structures and composite steel and concrete structures of buildings, Brazilian Association of Technical Standards, Rio de Janeiro, 2008.